Bull. Mater. Sci., Vol. 25, No. 4, August 2002, pp. 319–324. © Indian Academy of Sciences.

Impact toughness of high strength low alloy TMT reinforcement ribbed bar

BIMAL KUMAR PANIGRAHI* and SURENDRA KUMAR JAIN†

R&D Centre for Iron and Steel, Steel Authority of India Limited, Ranchi 834 002, India
†Steel Authority of India Ltd., Bhilai Steel Plant, Bhilai 490 001, India

MS received 12 April 2002

Abstract. Charpy V-notch impact toughness of 600 MPa yield stress TMT rebars alloyed with copper, phosphorus, chromium and molybdenum has been evaluated. Subsize Charpy specimens were machined from the rebar keeping the tempered martensite rim intact. The copper–phosphorus rebar showed toughness of 35 J at room temperature. The toughness of copper–molybdenum and copper–chromium rebars was 52 J. The lower toughness of phosphorus steel is attributed to solid solution strengthening and segregation of phosphorus to grain boundaries. Due to superior corrosion resistance, copper–phosphorus TMT rebar is a candidate material in the construction sector.

Keywords. Charpy impact toughness; TMT rebar; phosphorus; ductile–brittle transition; grain boundary segregation.

1. Introduction

Charpy impact testing is used for evaluation of impact toughness of a variety of mass-produced materials such as plate, forging, bar product, welded construction etc. ASTM standard (ASTM 1990) E23, other international standards and Indian standard (BIS 1988) IS1757 describe the procedure for specimen preparation and pendulum impact testing of metallic materials. This test is of great value for the selection of materials, quality control and as means of following the evolution of embrittlement. The advantages of Charpy testing are that it is a rapid test method requiring small investment, test specimens are of small size and simpler to machine (Wullaert 1970, 1974). The Charpy test data can be used to predict the performance of material in service condition. It reproduces the ductile to brittle transition of steel in about the same temperature range as it is actually observed in engineering structures. To nuclear scientists it is of great value in the study of irradiation related damage as the small size of the specimens makes it possible to introduce them in the reactor core without much difficulty. Through Charpy test the important data that can be generated are the absorbed energy, the ductile to brittle transition temperature (DBTT) for 50% cleavage fracture area and lateral contraction at the root of the notch (Pellini 1954) to measure ductility transition temperature (for 1% lateral contraction). The fractured Charpy specimens also give characteristic appearance of fracture surface. Unlike a few other tests, the strain rate is very high in the Charpy test. Table 1 shows the strain rate data (Mines 1989) of some fracture tests. The strain rate at the crack tip of a Charpy specimen can be as high as 6000–25,000 s^{-1} (Norris 1979; Tvergaard and Needleman 1986, 1988). Although the different specifications give details of Charpy testing, there is hardly any information on Charpy testing of TMT (thermomechanically treated) ribbed bar product, particularly the procedure to be followed in preparation of test specimens. In this context a study was undertaken to formulate a test procedure for Charpy testing of TMT rebar. In this paper the CVN impact toughness of some 600 MPa yield stress TMT rebars has been discussed with particular reference to the effects of phosphorus, molybdenum and chromium on toughness.

2. Materials and test procedures

Steel for high strength TMT rebar was produced in twin hearth furnace. The steel was cast into 9-tonne ingots. The ingots were processed to blooms (325 × 325 mm) and further to billets (100 × 100 mm). The billets were reheated at 1250°C and processed to TMT rebars of diameter 32 mm. The finish rolling temperature was ~ 1000°C. The TMT process involves cooling the rebar by pressurized water as it emerges from the finishing stand at a cooling rate higher than 200°C/s inside a THERMEX^{TM} water cooling installation so that a thin layer of martensite about 4 mm thick forms on the surface while the core is still austenite. On emergence out of the thermex unit, the bar is allowed to cool in the still air.

*Author for correspondence

Through this process, the martensitic rim gets self-tempered by the heat of the core as shown schematically in figure 1. Finally the core transforms to a relatively softer microstructure. Specimens for metallography were cut from the bar for examination of macro and microstructures after etching in 2% nital. The austenite grain size prior to water quenching in thermex unit was measured from the microstructure of the rim layer by linear intercept method. In order to evaluate the impact toughness, subsize specimens were prepared from the location shown in figure 2. The dimensions of a Charpy specimen are shown in figure 3. The preparation of subsize specimen by this method enabled preservation of the rim layer to a large extent so that after cutting the V-notch, about 2 mm layer of tempered martensite remained beneath the notch (figure 4). Triplicate specimens were tested at RT (+ 25°C), 0°C, – 20°C and – 40°C.

3. Results

The chemical composition of the TMT rebars is given in table 2. The phosphorus bearing TMT rebar had 0·093% phosphorus. The typical tensile properties of a TMT rebar were: yield stress, 605 MPa; UTS, 692 MPa and elongation, 19%. The macro and microstructures of the core and rim are shown in figure 5. The rim showed a tempered martensite structure. The core of Cu–P rebar was ferritic–pearlitic. The core inclusive of transition region of Cu–Mo and Cu–Cr rebars showed a mixed structure of polygonal ferrite, acicular ferrite, bainite, fine lamellar pearlite and carbide. The average austenite grain sizes of Cu–P, Cu–Mo and Cu–Cr steels were 96, 63 and 120 μm, respectively. Figure 6 shows the dependence of Charpy absorbed energy on temperature. The chromium and molybdenum steels showed similar values of absorbed energy (52 J) at RT. The absorbed energy of phosphorus steel was 35 J and 42 J at RT for 0·17% and 0·14% carbon

Table 1. Some common dynamic fracture tests with associated strain rates (after Mines 1989).

Type of test	$\dot{e}$ (s^{-1})	$\dot{k}_I$ ($MPa\sqrt{m}\cdot s^{-1}$)	V_0 ($m\cdot s^{-1}$)
Charpy test	10–1000	10^5–10^6	1–6
Three-point bend	0–10	Static – 10^5	0–15
Single point bend	102–1020	10^6–10^7	30–100
Compact tension	0–102	Static – 10^6	0–30

$\dot{e}$ = Strain rate; $\dot{k}_I$ = stress intensity rate; V_0 = velocity.

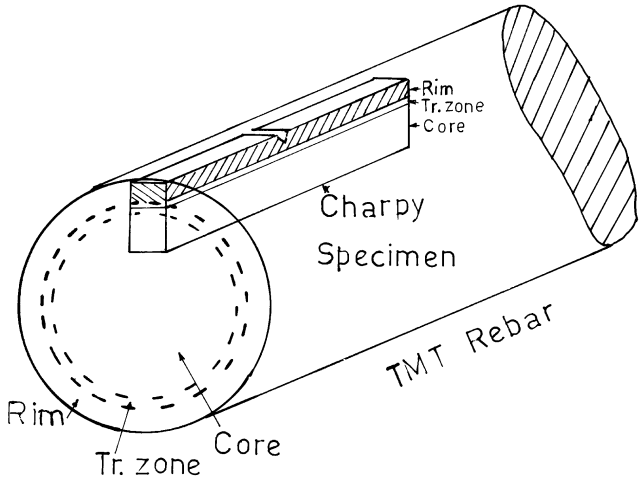

Figure 2. Location of charpy specimens.

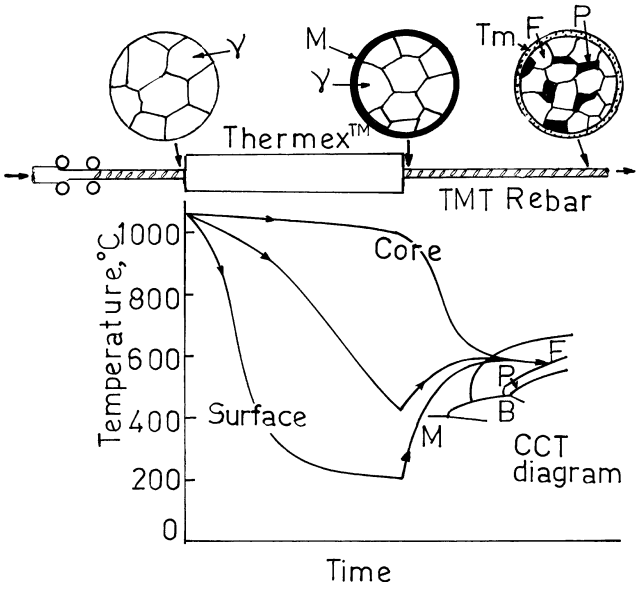

Figure 1. Schematic of TMT process (Tm: tempered martensite, P; pearlite, F: ferrite, B; bainite and g: austenite).

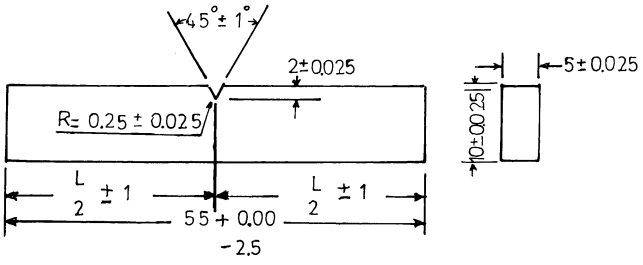

Figure 3. Dimensions of a Charpy specimen (all dimensions in mm).

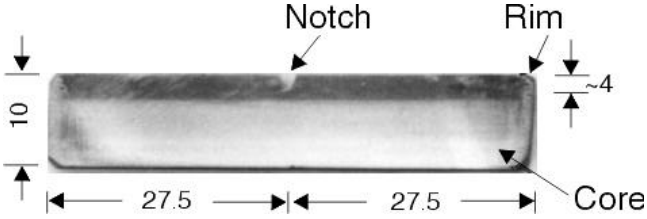

Figure 4. Charpy specimen after etching to show the tempered martensite rim and notch.

steel, respectively. While calculating DBTT, 50% of the maximum absorbed energy criterion was used. The DBTT calculated by this method gives the same result as of DBTT calculated from 50% of cleavage fracture area (Dahl 1992). The DBTT values of chromium and molybdenum steels were – 37°C and – 32°C, respectively while the phosphorus steel (0·17% C) showed a DBTT of + 4°C. The increase of DBTT for phosphorus steel is in

Table 2. Chemical composition (wt%) of TMT rebars.

	Composition										
Type of rebar	C	Mn	Si	S	P	Cu	Mo	Cr	Al	N	O
Cu–P	0·17	0·99	0·05	0·017	0·093	0·35	–	–	0·0025	0·0102	0·011
Cu–Mo	0·17	1·10	0·04	0·020	0·033	0·35	0·15	–	0·0026	0·0075	0·0102
Cu–Cr	0·21	1·04	0·04	0·019	0·020	0·34	–	0·49	0·0032	0·0096	0·0194
Cu–P	0·14	0·93	0·03	0·029	0·092	0·31	–	–	0·003	0·0118	0·0098

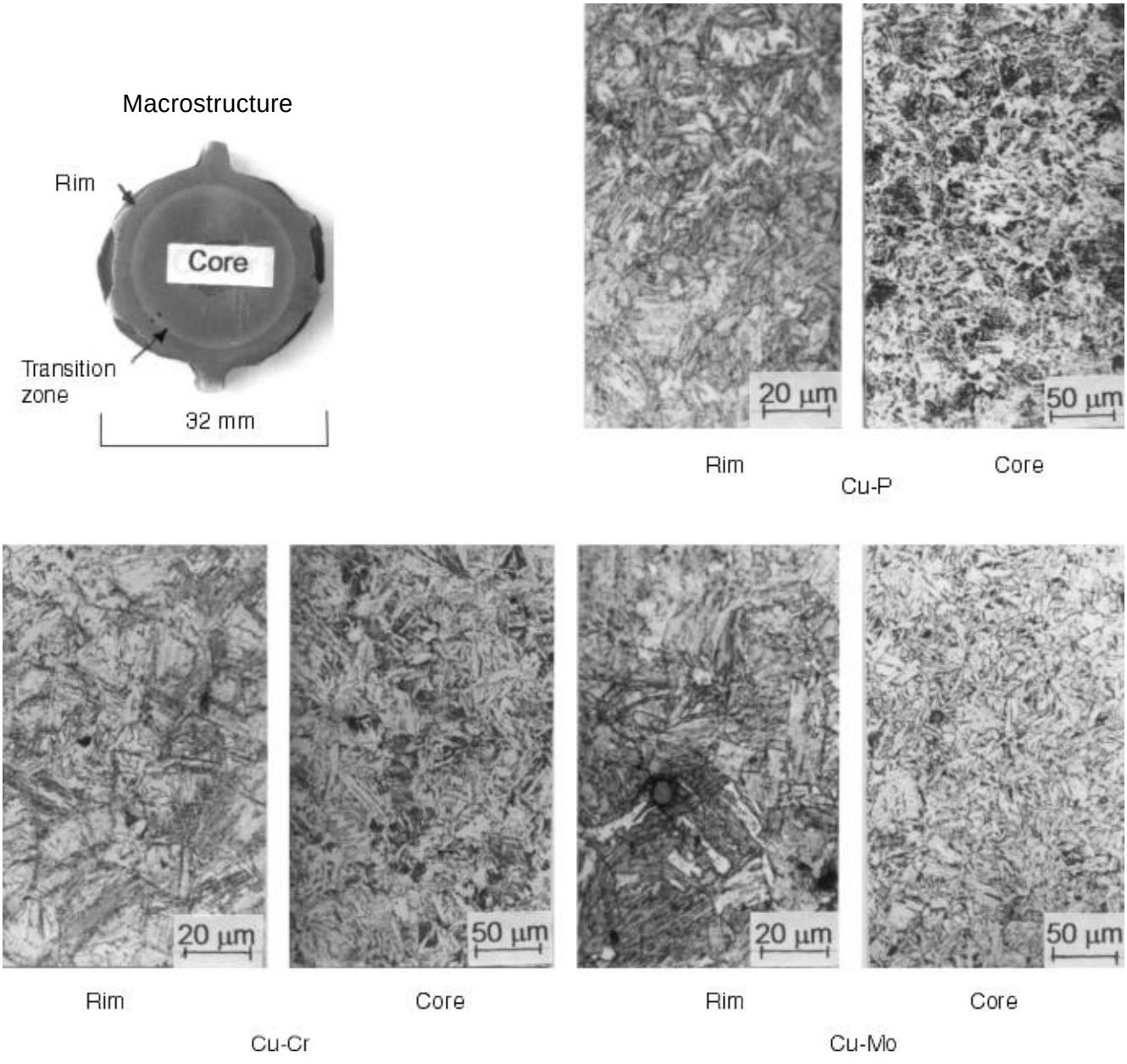

Figure 5. Rim and core structures of TMT rebar.

conformity with literature viz. each 0·01% increase of phosphorus, raised DBTT by + 7°C (McCallum 1999). With fall in test temperature, there has been an increase of absorbed energy for chromium steel at 0°C and – 20°C after which the absorbed energy drops to 18 J at – 40°C. In case of molybdenum and phosphorus steels, the absorbed energy decreased on lowering of test temperature.

4. Discussion and conclusions

It is well known that Charpy absorbed energy of hot rolled steel decreases with rise in carbon content due to increase of volume fraction of pearlite (NPC 1998). The rim of a TMT rebar resembles a low carbon quenched and tempered steel. As shown in the model (figure 7), on leaving the finishing stand at ~ 1000°C, a moderate austenite grain size (63–120 μm) is obtained (figure 7a) due to repeated recrystallization by rolling in roughing, intermediate and finishing stands (Panigrahi 2001). During quenching in the thermex unit a layer of lath martensite is formed (figure 7b) when *Ms* temperature is reached (Suzuki *et al* 2001). The martensite has high dislocation density (10^{14}–10^{15} lines/m^2) (Tsuchiyama *et al* 2001). Martensite being a supersaturated solution of carbon in *a*-iron is highly unstable. As the rebar emerges out of the thermex unit the rim temperature rises rapidly due to transfer of heat energy from the core and the martensite decomposes primarily to ferrite and carbide (figure 7c) lowering the dislocation density (Honeycombe 1981; Krauss 1995). The core which was austenitic on leaving the thermex unit got transformed to ferrite–pearlite (figures 1 and 7c) or a mixed structure of polygonal ferrite, acicular ferrite, lower bainite/upper bainite and fine pearlite depending on the temperature profile after quenching and chemical composition.

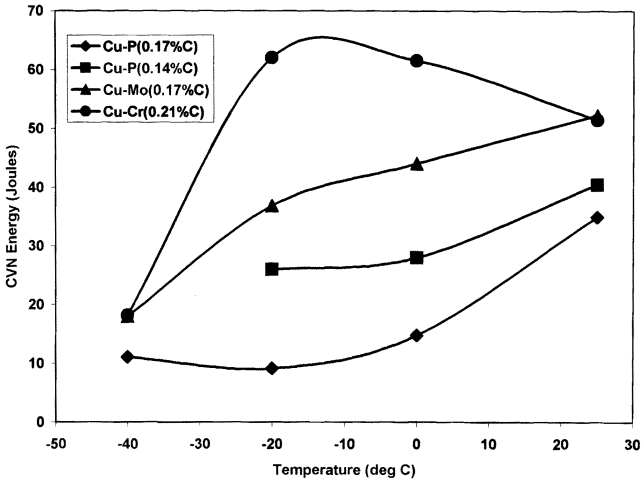

Figure 6. Dependence of CVN toughness on temperature.

In the molybdenum steel the DBTT was – 32°C. Molybdenum in solid solution raises the DBTT almost as fast as carbon (Dieter 1976). However, presence of mixed microstructures in the core (due to effect of molybdenum on austenite transformation) consisting of polygonal ferrite, acicular ferrite, lower bainite and fine pearlite had favourable effect on impact toughness viz. DBTT is lowered (Galibois *et al* 1979; Kalmykov *et al* 1984; Garcia de Andreas *et al* 2001).

Notwithstanding higher carbon content (0·21%) the chromium steel exhibited the lowest transition temperature (– 37°C). The reason for this could be a tempered martensite rim, a mixed microstructure in core and possibly due to anchoring of some free carbon atoms by chromium atoms (Houdremont 1956). Besides chromium also leads to decreased rate of segregation of carbon atoms at grain boundaries (Hornbogen 1970) which has a beneficial effect on DBTT.

Phosphorus steel (0·17% C) showed the highest DBTT (+ 4°C). Experimentally determined Fe–P phase diagram (Haughton 1927) and thermodynamic calculations (Ölsen 1949) have shown that a small amount of phosphorus can

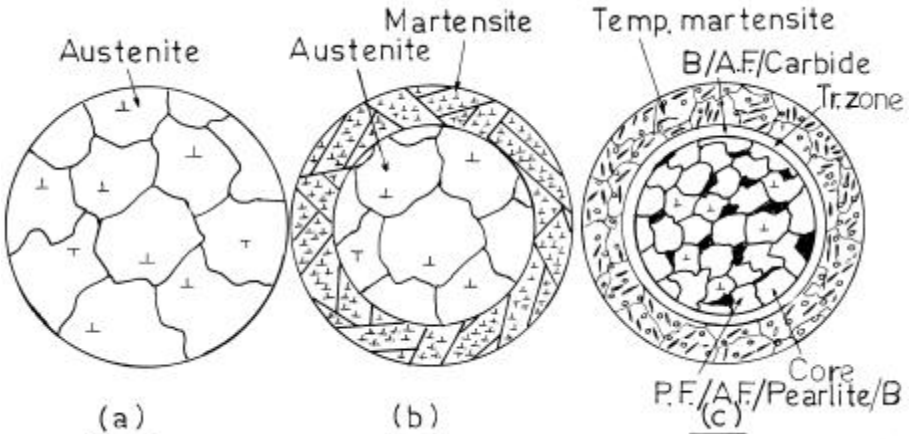

Figure 7. Model for evolution of microstructure in a TMT rebar (B: bainite, AF; acicular ferrite, PF: polygonal ferrite).

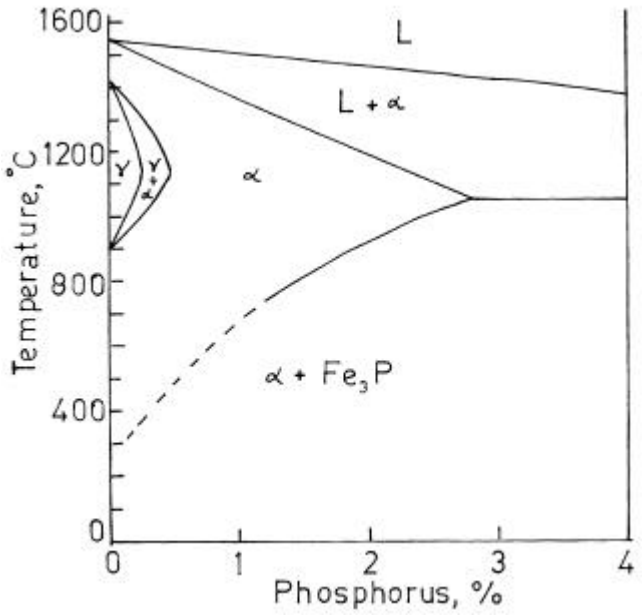

Figure 8. Phase diagram of Fe–P system.

dissolve in steel (figure 8) and increase the strength by solid solution hardening (Pickering 1978). Most steels contain not more than 0·05% phosphorus except the weather resistant steel which has 0·08–0·15% phosphorus. A larger amount of phosphorus increases DBTT due to segregation of phosphorus on grain boundaries. The reasons for segregation of phosphorus and associated embrittlement viz. higher DBTT, have been given by different investigators. White and Liu (1978) and Ermakov *et al* (2000) have concluded that lower value of absorbed energy of phosphorus steel and higher DBTT were due to its segregation tendency on grain boundaries which is due to greater diffusivity of phosphorus in *a*-iron (Gruzin and Minal 1964; Bruggerman and Roberts 1975; Pilling *et al* 1982). Segregated phosphorus atoms at grain boundaries lower the surface energy (Dieter 1976) and grain boundary cohesive energy (Briant and Messmer 1982) and make transmission of slip across grain boundary difficult (Nagumo *et al* 2000), thereby increasing the stress concentration that favours earlier initiation of brittle fracture (Biggs 1970). Consequently the energy necessary to cause fracture is lowered and DBTT is increased. Another reason for embrittlement could be due to electronegative effect. Phosphorus is electronegative according to Pauling's (1960) electronegativity scale with respect to host metal iron and draws charge from the host metal onto itself. As a result less charge is available to participate in the metal–to–metal bond viz. the bonding becomes weak or embrittling tendency is more. The weakening of the bond is more pronounced in the presence of some solutes like manganese which are less electronegative with respect to phosphorus. However, the observed toughness of phosphorus steel (0·17% C) is higher than conventional cold twisted and deformed semi-killed steel rebar (C 0·20–0·30%) and medium carbon hot rolled rebar (C 0·30–0·40%) used by the construction sector previously. The typical value of absorbed energy of full size Charpy specimens machined from cold twisted rebar was about 15 J at RT with DBTT around + 20°C. Lowering the carbon content of phosphorus steel to 0·14% improved the impact toughness (figure 6). In view of superior corrosion resistance of phosphorus TMT rebar, it is used increasingly in the construction sector.

References

American Society of Testing Materials 1990 *Annual book of ASTM Standards, Philadelphia 03.01* 197

Bureau of Indian Standards 1988 Indian Standards IS1757, New Delhi

Biggs W D 1970 in *Physical metallurgy* (ed.) R W Cahn (Amsterdam: North Holland Publishing Co.) p. 1217

Briant C L and Messmer R P 1982 *Acta Metall.* **30** 1811

Bruggerman G A and Roberts J A 1975 *Metall. Trans.* **A6** 755

Dahl W 1992 in *Steel I* (Dusseldorf: Springer Verlag, Verlag Stahl Eisen) p. 265

Dieter G 1976 *Mechanical metallurgy* (New York: McGraw Hill Book Co.) pp. 264, 498

Ermakov B S, Vologzhanina S A, Solntsev Y P and Kozachenko A V 2000 *Steel Trans.* **30** 72

Galibois A, Krishnadev M R and Dubey A 1979 *Metall. Trans.* **A10** 985

Garcia de Andreas, Capdevila C, Madariaga I and Gutierrez I 2001 *Scr. Mater.* **45** 709

Gruzin P L and Minal V V 1964 *Phys. Met. Metallogr. USSR* **17** 62

Haughton J L 1927 *J. Iron and Steel Inst.* **115** 417

Honeycombe R W K 1981 *Steel, microstructure and properties* (London: Edward Arnold; Ohio: American Society of Metals)

Hornbogen E 1970 in *Physical metallurgy* (ed.) R W Cahn (Amsterdam: North Holland Publishing Co.) p. 629

Houdremont E 1956 *Handbook of special steel* (Berlin: Springer Verlag) p. 630

Kalmykov V V, Volovik N G, Goncharenko N F, Dmitriev Y V and Shilovskaya E N 1984 *Steel USSR* **14** 551

Krauss G 1995 *Iron and Steel Inst. Jap. Int.* **35** 349

McCallum R 1999 *Iron and Steel Maker* **20** 67

Mines R A W 1989 in *Modern practice in stress and vibration analysis* (ed.) J E Motterschead (New York: Pergamon Press)

Nagumo M, Yagi T and Saitoh H 2000 *Acta Mater.* **48** 943

Norris D M 1979 *Eng. Fract. Mech.* **11** 261

NPC Information 1998 (Dusseldorf: Niobium Products Corporation)

Ölsen W 1949 *Stahl Eisen* **69** 468

Panigrahi B K 2001 *Bull. Mater. Sci.* **24** 361

Pauling L 1960 in *The nature of the chemical bonds* (Ithaca, New York: Cornell University Press) p. 93

Pellini W S 1954 in *ASTM special technical publication, No. 158* (Philadelphia: ASTM) p. 216

Pickering F B 1978 *Physical metallurgy and design of steels* (London: Applied Science Publisher) Ch. 4

Pilling J, Ridley N and Gooch D J 1982 *Acta Metall.* **30** 1587

Suzuki T, Shimono M and Kajiwara S 2001 *Mater. Sci. Engg.* **A312** 104

Tsuchiyama T, Miyamoto Y and Takai S 2001 *Iron and Steel Inst. Jap. Int.* **41** 1047

Tvergaard V and Needleman A 1986 *J. Mech. Phys. Solids* **34** 213

Tvergaard V and Needleman A 1988 *Int. J. Fract.* **37** 197

White C L and Liu T 1978 *Scr. Metall.* **12** 727

Wullaert R A 1970 in *Impact testing of materials, ASTM STP-466* (Philadelphia: ASTM) p. 148

Wullaert R A 1974 in *Fracture prevention and control* (ed.) D W Hoeppner (Ohio: ASM) p. 255